



HAL
open science

Photomodulation of Charge Transport in All-Semiconducting 2D–1D van der Waals Heterostructures with Suppressed Persistent Photoconductivity Effect

Zhaoyang Liu, Haixin Qiu, Can Wang, Zongping Chen, Björn Zyska, Akimitsu Narita, Artur Ciesielski, Stefan Hecht, Lifeng Chi, Klaus Müllen, et al.

► **To cite this version:**

Zhaoyang Liu, Haixin Qiu, Can Wang, Zongping Chen, Björn Zyska, et al.. Photomodulation of Charge Transport in All-Semiconducting 2D–1D van der Waals Heterostructures with Suppressed Persistent Photoconductivity Effect. *Advanced Materials*, 2020, pp.2001268. 10.1002/adma.202001268 . hal-02917281

HAL Id: hal-02917281

<https://hal.science/hal-02917281>

Submitted on 18 Aug 2020

HAL is a multi-disciplinary open access archive for the deposit and dissemination of scientific research documents, whether they are published or not. The documents may come from teaching and research institutions in France or abroad, or from public or private research centers.

L'archive ouverte pluridisciplinaire **HAL**, est destinée au dépôt et à la diffusion de documents scientifiques de niveau recherche, publiés ou non, émanant des établissements d'enseignement et de recherche français ou étrangers, des laboratoires publics ou privés.

DOI: 10.1002/((please add manuscript number))

Article type: Communication

Photo-Modulation of Charge Transport in all-semiconducting 2D-1D van der Waals Heterostructures with Suppressed Persistent Photoconductivity Effect

*Zhaoyang Liu, † Haixin Qiu, † Can Wang, Zongping Chen, Björn Zyska, Akimitsu Narita, Artur Ciesielski, Stefan Hecht, Lifeng Chi, Klaus Müllen, Paolo Samori**

†These authors contributed equally to this work.

Dr. Z. Liu, H. Qiu, Dr. C. Wang, Dr. A. Ciesielski, Prof. Dr. P. Samori
Université de Strasbourg and CNRS, ISIS, 8 allée Gaspard Monge, 67000 Strasbourg, France
*Corresponding author: samori@unistra.fr

B. Zyska, Prof. Dr. S. Hecht
Department of Chemistry and IRIS Adlershof, Humboldt-Universität zu Berlin, 12489, Berlin

Prof. Dr. S. Hecht
Germany, DWI - Leibniz Institute for Interactive Materials, Forckenbeckstr. 50, 52056
Aachen, Germany, & Institute of Technical and Macromolecular Chemistry, RWTH Aachen
University, Worringer Weg 2, 52074 Aachen, Germany

Dr. Z. Chen, Dr. A. Narita, Prof. Dr. K. Müllen
Max Planck Institute for Polymer Research, Ackermannweg 10, 55128 Mainz, Germany

Asst. Prof. Dr. A. Narita
Organic and Carbon Nanomaterials Unit, Okinawa Institute of Science and Technology
Graduate University, 1919-1 Tancha, Onna-son, Kunigami, Okinawa 904-0495, Japan

Prof. Dr. L. Chi
Jiangsu Key Laboratory for Carbon Based Functional Materials & Devices, Institute of
Functional Nano & Soft Materials (FUNSOM), Soochow University, Suzhou 215123, P. R.
China

Keywords: two-dimensional semiconductor, graphene nanoribbon, van der Waals heterostructure, photo-modulation, persistent photoconductivity

Abstract

Van der Waals heterostructures (VDWHs), obtained *via* the controlled assembly of two-dimensional atomically thin crystals, exhibit unique physico-chemical properties, rendering them prototypical building blocks to explore new physics and for applications in optoelectronics. As the emerging alternatives to graphene, monolayer transition metal dichalcogenides and *bottom-up* synthesized graphene nanoribbons (GNRs) are promising candidates for overcoming the shortcomings of graphene, such as the absence of a bandgap in its electronic structure, which is essential in optoelectronics. Herein, VDWHs comprising GNRs onto monolayer MoS₂ are fabricated. Field-effect transistors (FETs) based on such VDWHs show an efficient suppression of the persistent photoconductivity typical of MoS₂, resulting from the interfacial charge transfer process. The MoS₂-GNR FETs exhibit drastically reduced hysteresis and more stable behavior in the transfer characteristics, which is a prerequisite for the further photo-modulation of charge transport behavior within the MoS₂-GNR VDWHs. The physisorption of photochromic molecules onto the MoS₂-GNR VDWHs enables reversible light-driven control over charge transport. In particular, the drain current of the MoS₂-GNR FET can be photo-modulated by 52%, without displaying significant fatigue over at least 10 cycles. Moreover, four distinguishable output current levels can be achieved, demonstrating the great potential of MoS₂-GNR VDWHs for multilevel memory devices.

Graphene, the archetypal two-dimensional (2D) crystal, has been the target of both extensive fundamental studies and numerous technological advancements during the last 15 years.^[1] Graphene is an extremely promising material for future generation of flexible/wearable high speed optoelectronics by taking advantage of its extraordinary physical properties, including its ultra-high charge carrier mobility at room temperature, its outstanding mechanical robustness and its high light transmittance in the visible range.^[2] However, the absence of a bandgap in its electronic structure does not enable graphene to be switched off in field-effect transistors (FETs) based logic circuits.^[1, 3] The most promising and straightforward strategy for opening the bandgap in graphene relies on mastering quantum confinement effect *via* the synthesis of graphene nanoribbons (GNRs), which are narrow strips of graphene with atomically precise topology.^[4] The electronic properties of GNRs are critically dependent on their width and edge structure, thus they can be tuned *via* the ad-hoc design of the synthetic precursor.^[5] Recent ground-breaking studies of on-surface synthesis both under ultra-high-vacuum (UHV)^[6] and by chemical vapor deposition (CVD)^[7] demonstrated the versatility of such *bottom-up* approach to generate a wide library of GNRs exhibiting excellent photo-conductivities while maintaining adjustable electronic bandgaps. Such features make these systems highly promising for future optoelectronics based on low-dimensional nanomaterials^[3b, 8] (*e.g.* 0D, 1D, and 2D etc.).

The alternative strategy which has been pursued to overcome the lack of bandgap in graphene widens the focus to a broadest variety of 2D layered materials exhibiting diverse chemical structure and composition. The resulting electronic properties can range from insulators, semiconductors to conductors.^[3b, 9] Among them, monolayer 2D transition-metal dichalcogenides (TMDCs), whose bandgap can be finely tuned, represent promising alternatives to graphene for applications in nanophotonics, nanoelectronics, nanoscale sensing and actuation, in the post-silicon era.^[10] So far, MoS₂ is the most extensively studied TMDC because of its robustness and high charge carrier mobility.^[3a, 9a, 11] However, a major

drawback of MoS₂ and related hybrid structures for applications in optoelectronics is its persistent photoconductivity (PPC) effect,^[12] which is defined as the light-induced enhancement in conductivity that persists for a long period after termination of photoexcitation,^[13] *i.e.* the device cannot be totally switched off in the dark. Suppressing the PPC effect is therefore of utmost importance to leverage the fundamental features of MoS₂ for various technological applications.^[14]

The TMDCs' properties can be "corrected" and optimized *via* the atomically controlled formation of van der Waals heterostructures (VDWHs),^[15] by taking full advantage of the versatility of interfacing low-dimensional nanostructures without the constraints of crystal lattice matching.^[3b] Hitherto, VDWHs have been primarily fabricated by superimposing two different types of 2D materials.^[15b] Little has been done on forming VDWHs by superimposing nanostructures with different dimensionalities. In particular, the combination of 2D with 1D systems has been attempted to combine 2D graphene flakes with 1D dielectrics or conductors.^[16] All-semiconducting 2D-1D VDWHs have not been properly addressed for applications in optoelectronics. The large library of recently developed 1D semiconductors, in particular based on suitably designed GNRs, open new avenues for explorations in the field of VDWHs.^[17] Moreover, the modulation of the charge transport behavior of the VDWHs using different external stimuli is highly appealing for imparting them new functions. This should ultimately allow diverse applications based on novel stimuli responsive systems.^[18]

Herein, we fabricate a VDWHs by depositing 1D GNRs onto 2D MoS₂, to achieve an effective suppression of the PPC effect of MoS₂ as a result of interfacial charge transfer process. The hysteresis of the MoS₂-GNR FETs decreases significantly as compared to MoS₂ based FETs, and the transfer curves become more stable upon switching between 530 nm light irradiation and dark conditions. The reduction of the PPC effect is also evidenced in dynamic photoresponse analysis: the dark current value after illumination in FET based on

MoS₂-GNR VDWH displays only 3% enhancement, being about one order of magnitude lower than the case of pristine MoS₂ FET. Such a minimal enhancement represents a prerequisite to monitor distinguishable current signal changes determined by light inputs, *e.g.* when photochromic molecular systems are integrated in the device. The molecular functionalization of MoS₂-GNR VDWH is achieved through physisorption rather than chemisorption. Although chemisorption of reactive molecules typically leads to more robust hybrid systems as compared to physisorption, the former could be detrimental for the overall electronic properties of MoS₂ nanosheets, thereby irreversibly affecting the electrical characteristics of MoS₂-GNR VDWH. Therefore, the less invasive physisorption approach is employed. A physisorbed photochromic spiropyran monolayer enabled a reversible remote-control of the charge transport in MoS₂-GNR FET, by exploiting the change in dipole moment between the two photo-isomers states acting as light activated gate. The photo-modulation of the source-drain current in MoS₂-GNR FET can be as high as 52%, which is durable without showing significant fatigue over at least 10 cycles. Moreover, upon varying the light irradiation period, four distinguishable output current levels could be achieved accordingly, which demonstrates the great potential of functionalized MoS₂-GNR VDWH as prototypical active component in multilevel memory devices.

In order to assemble the VDWHs based on MoS₂-GNR, monolayer MoS₂ is first isolated *via* micro-mechanical exfoliation from bulk MoS₂ crystal, followed by its transfer onto a SiO₂/Si substrate. GNRs with an armchair type edge structure and 7 carbon atoms in width (7-AGNR) are grown on Au/SiO₂ substrates under ultrahigh vacuum conditions, starting from 10,10'-dibromo-9,9'-bianthryl, which undergoes polymerization and cyclodehydrogenation at 200 °C and 400 °C, respectively.^[6b, 7d] The 7-AGNR film is then transferred on top of the MoS₂ chip by a well-established poly(methyl methacrylate) (PMMA) supporting layer assisted lift-off and film transfer approach,^[7b] yielding the VDWH architecture portrayed in **Figure 1a**. Since the electronic properties of MoS₂ are highly

sensitive to the influence of its surrounding environment due to the unique atomically thin 2D structure, Raman and photoluminescence (PL) spectroscopy are employed to prove the formation of MoS₂-GNR VDWH, as well as to monitor the electronic interactions between MoS₂ and 7-AGNR. The Raman spectra of the pristine MoS₂ flake (measured under 532 nm laser, Figure 1b) displays two characteristic first-order phonon modes, i.e. the in-plane oscillation E_{2g}¹ mode and the out-of-plane oscillation A_{1g} mode. The peaks which are located at 384.8 cm⁻¹ and 403.9 cm⁻¹, thus having a ~19 cm⁻¹ wavenumber difference, confirm the monolayer nature of the employed MoS₂ flake.^[19] It has been proved that for the monolayer MoS₂, the A_{1g} mode is more sensitive to the charge carrier doping level due to a stronger electron-phonon coupling, whereas the E_{2g}¹ mode is more sensitive to strain due to the breaking of symmetry. Raman spectroscopy has also emerged as a powerful technique to study the vibrational modes for the sp²-hybridized carbon nanomaterials. When a 7-AGNR film is placed on the top of the same monolayer MoS₂ flake, forming a network of 7-AGNRs covering the surface of MoS₂ to realize the VDWH architecture, four peaks located between 1608 cm⁻¹ and 1219 cm⁻¹ appear, which can be assigned to G, D, and edge C-H peaks typical of graphene, respectively.^[7b] More importantly, the sharp peak located at 395 cm⁻¹ is the characteristic width-specific radial breathing-like mode (RBLM) peak, proving the structure of 7-AGNR. Since the RBLM is resonantly excited for photon energies near the lowest optical transitions of 7-AGNR, green laser (532 nm, 2.33 eV) is thus employed to just slightly exceed the optical gap of 7-AGNR (2.1 eV). Meanwhile, as the RBLM frequency varies strongly with GNR width, the sharp peak at 395 cm⁻¹ corresponding to a width of 0.74 nm further illustrates the high uniformity in the width at the atomic level of *bottom-up* on-surface synthesized 7-AGNR. It is worth noting that the Raman spectroscopy is performed based on the 7-AGNR sample transferred from Au onto SiO₂ substrate with MoS₂ flakes. These Raman peaks are in excellent agreement with the calculated values *via* density functional theory, thereby demonstrating the high quality of the obtained 7-AGNR sample as well as the preserved

structural integrity of the film after the transfer process.^[6b] Moreover, the blue shift of the A_{1g} phonon mode of MoS_2 by $\sim 1 \text{ cm}^{-1}$ suggests the p-type doping effect of MoS_2 by the addition of 7-AGNR.^[20] PL spectra of both pristine MoS_2 and MoS_2 -GNR VDWH are shown in Figure 1c, with the low-energy (A) exciton varies significantly over the spectral range of 1.8-2.0 eV. Since the A-exciton of monolayer MoS_2 includes both neutral excitons (X) and trions (negatively charged excitons, X^-), the trion spectral weight can be correlated to the doping level of MoS_2 .^[21] The fitted peaks suggest that the spectral weight of the trion in the MoS_2 -GNR VDWH is significantly lower than those in pristine MoS_2 . This feature results from the typical intrinsic n-type doping of MoS_2 as well as the possible p-type doping effect of MoS_2 by 7-AGNR, in accordance with the Raman results.^[14] Such interfacial charge transfer regime within MoS_2 -GNR VDWH under light irradiation might be beneficial for the overall optoelectronic properties.^[22]

To cast light onto the optoelectronic properties of the MoS_2 -GNR VDWHs, they have been integrated as the channel material into the back-gated FET device (schematic device geometry shown in Figure 1a), with top source-drain electrodes (60 nm thick gold) produced by a standard photolithography process. Because of the limited lateral size of the obtained monolayer MoS_2 flakes exfoliated *via* the scotch tape method we opted to use the two-point probe geometry rather than four-point probe. The former geometry is widely employed to study the photoconductivity in MoS_2 devices.^[3a, 9a, 11, 23] As a control experiment, a back-gated FET based on pristine MoS_2 is also fabricated. **Figure 2a** and b shows the transfer electrical characteristics (I_{ds} - V_g) of the FETs based on pristine MoS_2 and MoS_2 -GNR VDWH measured under dark condition, plotted in both linear and logarithmic scale, while the source-drain voltage V_{ds} is kept at 1 V. The hysteresis on such transfer curves is investigated by recording consecutive forward and reverse sweeps. The FET based on pristine MoS_2 reveals a significant hysteresis width of 5.2 V, which is a common feature attributed to the presence of trap states either on the MoS_2 surface (possible charge transfer from/to absorbed molecules)

or at the MoS₂/SiO₂ interface.^[3a, 24] By comparison, the FET based on MoS₂-GNR VDWH displays a drastically smaller hysteresis width of 1.4 V. Such an improvement is directly correlated to the better interface between MoS₂ and 7-AGNR and possible encapsulation effects of 7-AGNR film, which is characterized by a severe reduction of trap states. In order to determine the possible PPC effect of pristine MoS₂, the linear I_D-V_G characteristics of the FET are also measured under both dark and 530 nm illumination conditions, by performing over 50 cycles of such dark-illumination tests to gain insight into device stability toward light irradiation. As shown in Figure 2c, the dark current rises significantly with increased cycling number. From the 2nd cycle, the shape of the dark current curve begins to bend toward the high current direction, under the same V_g and V_{ds}, the current value enhances, thus the resistance decreases and conductivity increases. Such light-induced enhancement in conductivity persisting for a long period after the termination of illumination behavior is in accordance with the definition of PPC effect.^[3a, 13] This pronounced PPC effect would influence the determination of the photocurrent value due to instability of the dark current, and is therefore detrimental to further applications of MoS₂ FET in optoelectronics. Conversely, the I_{ds}-V_g characteristics of FET based on MoS₂-GNR VDWH are much more stable when undergoing 50 cycles of such dark-illumination tests than the case of pristine MoS₂ FET, as shown in Figure 2d. The dark current varies only in a small range, which demonstrates the suppressed PPC effect by the addition of 7-AGNR to MoS₂. Such phenomenon is attributed to the charge transfer regime within the interface of MoS₂-GNR VDWH, *i.e.* the photogenerated electrons of MoS₂ are more favorable to be transferred into 7-AGNR, rather than filling the trap states on the MoS₂ surface or getting localized at the MoS₂/SiO₂ interface.

A dynamic photoresponse study of I_{ds} at 0 V of gate voltage was also performed to better compare the PPC effect of the two FETs based on pristine MoS₂ and MoS₂-GNR VDWH. **Figure 3** displays the comparison of the dynamic current variation under dark and

530 nm illumination conditions. When illumination is on, the I_{ds} in both two cases exhibits a sudden increase, which can be attributed to the photogenerated charge carriers. Once the light is turned off, the current of a pristine MoS₂ FET is not fully recovered to the original value, being significantly higher than the adjacent dark current level with 36% enhancement. This is unambiguous evidence of the PPC effect. In contrast, the dark current value after illumination in FET based on MoS₂-GNR VDWH displays only 3% enhancement, being about one order of magnitude lower than the case of pristine MoS₂ FET. The successful suppression of the PPC effect represents a milestone for further functionalization of the 1D-2D VDWH with light sensitive molecules.

Aiming at tuning the charge transport through the VDWHs, therefore enabling multifunctional control over the output current signals, the interfacing of 2D materials and hybrids thereof with photo-responsive molecular systems provides an efficient and versatile approach to achieve different charge carrier doping levels, ultimately leading to a reversible modulation of the electronic properties of the VDWHs.^[10a, 18c, 25] As a proof-of-concept, we have physisorbed a top layer of photochromic spiropyran (SP-C18) molecules and we explored the photo-modulation of the charge transport through MoS₂-GNR VDWH (**Figure 4a**). The initial device without SP-C18 molecules exhibits unipolar n-type behavior with pristine electron mobility of 21.4 cm² V⁻¹ s⁻¹. Figure 4b shows that the presence of SP-C18 ad-molecules induces an increase of drain current I_{ds} and a negative shift of threshold voltage ($\Delta V_{th} = -1.9$ V), indicating a minor n-type doping effect by the SP-C18 molecules. After UV irradiation of the whole FET channel, the closed ring SP-C18 isomer is converted to the opening merocyanine (MC-C18) form, accompanied by a large variation of the molecular dipole moment, which induces a major increase of current and a continuous downshift of threshold voltage $\Delta V_{th} = -4.1$ V (Figure 4c). Therefore, the MC-C18 molecules further strengthen the n-type doping effect of MoS₂-GNR VDWH, with a significantly enhanced carrier concentration of 9.7×10^{11} cm⁻². The estimated sheet carrier density amounts to 3.8×10^{12} cm⁻².

² and $4.8 \times 10^{12} \text{ cm}^{-2}$ for MoS₂-GNR FET with SP-C18 molecules before and after UV irradiation.^[26] The current modulation induced by the SP-C18/MC-C18 photo-switching is calculated to be around 52%. By subsequent visible light irradiation, the reverse process takes place and all these electrical properties restore to the original values. Therefore, by programming the molecules into different states, the FET devices exhibit different electrical transport behavior. In total 10 illumination cycles are launched to investigate the stability of such light-induced current modulation. In Figure 4d, we plot the normalized current values obtained from the transfer curves at $V_g = 30 \text{ V}$, which proves a good stability and reversibility of our device system. Figure S1 displays the output characteristics of the MoS₂-GNR FET with SP-C18/MC-C18 molecules. It exhibits a linear and symmetric relationship between I_{ds} and drain biases V_{ds} , proving a low contact resistance with the electrodes. As a control experiment, transfer characteristics are recorded in both the dark and after UV/vis illumination on MoS₂-GNR FET device without SP-C18 molecules (Figure S2). It displays no obvious variation, thus proving that the SP-C18 molecules are responsible for the current modulation. To demonstrate the importance of a suppressed PPC effect, another control experiment on pristine MoS₂ FET device coated with SP-C18 molecules is performed. As shown in Figure S3, an increase of current can be observed after UV irradiation, but the current can only be partially restored to the original value after irradiation with visible light. This phenomenon is attributed to the fact that the PPC effect hinders the observation of the molecule-induced modulation. The dynamic evolution of current under alternative dark and UV/vis illumination conditions is portrayed in Figure 4e. When UV light is on (red boxed region), the current has a swift increase due to the photocurrent followed by a further yet gradual increase which is resulting from the SP-C18 to MC-C18 switching. The current level is higher than original curves when UV light is off, in accordance with the results obtained in the transfer measurement. Under visible light (blue boxed region), apart from the photocurrent, the current displays a gradual decrease which can be attributed to the MC-C18 to SP-C18

relaxation. The current level returns to the original value after one switching cycle. For the sake of comparison, control experiments on a MoS₂-GNR FET device without SP-C18 molecules are performed under the same illumination conditions. As displayed in Figure S4, the current reveals photoresponse under both UV and vis illumination, whereas it does not evidence any significant modulation after the illumination. In Figure 4f, we present a multilevel current obtained by exposing the device to a periodic short time UV illumination. The current level is proportional to the SP-C18/MC-C18 population ratio, therefore by controlling the irradiation time, the device can reach different current levels. At the end of each UV illumination, the current level shows a distinguishable increase compared with adjacent levels and the value remains stable. Upon 4 subsequent UV irradiations the device reaches 4 different current levels and as a result of the final long-time visible light irradiation enables the current to recover its original state, demonstrating its potential as multibit nonvolatile memories.

In conclusion, the fabrication of mixed-dimensional VDPWH based on 1D 7-AGNR onto 2D MoS₂ represents an efficient strategy to suppress the PPC effect of MoS₂ due to the presence of interfacial charge transfer process, as evidenced by a 3-fold reduction of the hysteresis width, and more stable transfer characteristics upon switching between light irradiation and dark conditions. Such a platform is therefore ideal to photo-modulate the charge transport in MoS₂-GNR FET when decorated with physisorbed photochromic molecules. The drain current of the MoS₂-GNR FET can be photo-modulated by 52%, and four distinguishable output current levels can be achieved, demonstrating the great potential of MoS₂-GNR VDPWH for multilevel memory devices. These results may pave the way toward ultra-thin multifunctional optoelectronics for logic-gates in the framework of integrating “More than Moore” technologies (analog functions, such as sensor, biochips, etc.) into CMOS digital circuits.

Supporting Information

Supporting Information is available from the Wiley Online Library or from the author.

Acknowledgements

The authors sincerely acknowledge funding from the European Commission through the ERC projects SUPRA2DMAT (GA-833707) and Light4Function (GA-308117), the Graphene Flagship Core 2 project (GA-785219), the Marie Skłodowska-Curie projects ITN project iSwitch (GA-642196) and ULTIMATE (GA-813036), the M-ERA.NET project MODIGLIANI, the Agence Nationale de la Recherche through the Labex projects CSC (ANR-10-LABX-0026 CSC) and NIE (ANR-11-LABX-0058 NIE) within the Investissement d'Avenir program (ANR-10-120 IDEX-0002-02), the International Center for Frontier Research in Chemistry (icFRC), the Max Planck Society, the German Research Foundation (DFG – Projektnummer 182087777 – SFB 951) as well as the Chinese Scholarship Council.

Received: ((will be filled in by the editorial staff))

Revised: ((will be filled in by the editorial staff))

Published online: ((will be filled in by the editorial staff))

References

- [1] K. S. Novoselov, V. I. Falko, L. Colombo, P. R. Gellert, M. G. Schwab, K. Kim, *Nature* **2012**, *490*, 192.
- [2] a) J. Du, S. Pei, L. Ma, H.-M. Cheng, *Adv. Mater.* **2014**, *26*, 1958; b) F. Bonaccorso, Z. Sun, T. Hasan, A. C. Ferrari, *Nat. Photonics* **2010**, *4*, 611; c) N. O. Weiss, H. Zhou, L. Liao, Y. Liu, S. Jiang, Y. Huang, X. Duan, *Adv. Mater.* **2012**, *24*, 5782.
- [3] a) W. Zhang, J.-K. Huang, C.-H. Chen, Y.-H. Chang, Y.-J. Cheng, L.-J. Li, *Adv. Mater.* **2013**, *25*, 3456; b) Y. Liu, N. O. Weiss, X. Duan, H.-C. Cheng, Y. Huang, X. Duan, *Nat. Rev. Mater.* **2016**, *1*, 16042; c) F. Schwierz, *Nat. Nanotechnol.* **2010**, *5*, 487.

- [4] a) A. Narita, Z. Chen, Q. Chen, K. Müllen, *Chem. Sci.* **2019**, *10*, 964; b) X.-Y. Wang, A. Narita, K. Müllen, *Nat. Rev. Chem.* **2017**, *2*, 0100.
- [5] a) L. Talirz, P. Ruffieux, R. Fasel, *Adv. Mater.* **2016**, *28*, 6222; b) A. Narita, X. Feng, K. Müllen, *Chem. Rec.* **2015**, *15*, 295; c) A. Narita, X.-Y. Wang, X. Feng, K. Mullen, *Chem. Soc. Rev.* **2015**, *44*, 6616.
- [6] a) J. Cai, C. A. Pignedoli, L. Talirz, P. Ruffieux, H. Söde, L. Liang, V. Meunier, R. Berger, R. Li, X. Feng, K. Müllen, R. Fasel, *Nat. Nano.* **2014**, *9*, 896; b) J. Cai, P. Ruffieux, R. Jaafar, M. Bieri, T. Braun, S. Blankenburg, M. Muoth, A. P. Seitsonen, M. Saleh, X. Feng, K. Mullen, R. Fasel, *Nature* **2010**, *466*, 470; c) P. Ruffieux, S. Wang, B. Yang, C. Sánchez-Sánchez, J. Liu, T. Dienel, L. Talirz, P. Shinde, C. A. Pignedoli, D. Passerone, T. Dumschlaff, X. Feng, K. Müllen, R. Fasel, *Nature* **2016**, *531*, 489; d) X. Zhou, G. Yu, *Adv. Mater.* **2020**, *32*, 1905957.
- [7] a) Z. Chen, H. I. Wang, N. Bilbao, J. Teyssandier, T. Pechtl, N. Cavani, A. Tries, R. Biagi, V. De Renzi, X. Feng, M. Kläui, S. De Feyter, M. Bonn, A. Narita, K. Müllen, *J. Am. Chem. Soc.* **2017**, *139*, 9483; b) Z. Chen, H. I. Wang, J. Teyssandier, K. S. Mali, T. Dumschlaff, I. Ivanov, W. Zhang, P. Ruffieux, R. Fasel, H. J. Räder, D. Turchinovich, S. De Feyter, X. Feng, M. Kläui, A. Narita, M. Bonn, K. Müllen, *J. Am. Chem. Soc.* **2017**, *139*, 3635; c) Z. Chen, W. Zhang, C.-A. Palma, A. Lodi Rizzini, B. Liu, A. Abbas, N. Richter, L. Martini, X.-Y. Wang, N. Cavani, H. Lu, N. Mishra, C. Coletti, R. Berger, F. Klappenberger, M. Kläui, A. Candini, M. Affronte, C. Zhou, V. De Renzi, U. del Pennino, J. V. Barth, H. J. Räder, A. Narita, X. Feng, K. Müllen, *J. Am. Chem. Soc.* **2016**, *138*, 15488; d) H. Sakaguchi, Y. Kawagoe, Y. Hirano, T. Iruka, M. Yano, T. Nakae, *Adv. Mater.* **2014**, *26*, 4134; e) H. Sakaguchi, S. Song, T. Kojima, T. Nakae, *Nat. Chem.* **2016**, *9*, 57.
- [8] R. Khare, D. B. Shinde, S. Bansode, M. A. More, M. Majumder, V. K. Pillai, D. J. Late, *Appl. Phys. Lett.* **2015**, *106*, 023111.

- [9] a) O. Lopez-Sanchez, D. Lembke, M. Kayci, A. Radenovic, A. Kis, *Nat. Nanotechnol.* **2013**, *8*, 497; b) X. Zhuang, Y. Mai, D. Wu, F. Zhang, X. Feng, *Adv. Mater.* **2015**, *27*, 403; c) P. Ranjan, T. K. Sahu, R. Bhushan, S. S. Yamijala, D. J. Late, P. Kumar, A. Vinu, *Adv. Mater.* **2019**, *31*, 1900353.
- [10] a) S.-L. Li, K. Tsukagoshi, E. Orgiu, P. Samori, *Chem. Soc. Rev.* **2016**, *45*, 118; b) S. Manzeli, D. Ovchinnikov, D. Pasquier, O. V. Yazyev, A. Kis, *Nat. Rev. Mater.* **2017**, *2*, 17033; c) D. Jariwala, V. K. Sangwan, D. J. Late, J. E. Johns, V. P. Dravid, T. J. Marks, L. J. Lauhon, M. C. Hersam, *Appl. Phys. Lett.* **2013**, *102*, 173107; d) S. Ratha, A. J. Simbeck, D. J. Late, S. K. Nayak, C. S. Rout, *Appl. Phys. Lett.* **2014**, *105*, 243502; e) D. J. Late, Y.-K. Huang, B. Liu, J. Acharya, S. N. Shirodkar, J. Luo, A. Yan, D. Charles, U. V. Waghmare, V. P. Dravid, C. N. R. Rao, *ACS Nano* **2013**, *7*, 4879.
- [11] Z. Yin, H. Li, H. Li, L. Jiang, Y. Shi, Y. Sun, G. Lu, Q. Zhang, X. Chen, H. Zhang, *ACS nano* **2012**, *6*, 74.
- [12] Y.-C. Wu, C.-H. Liu, S.-Y. Chen, F.-Y. Shih, P.-H. Ho, C.-W. Chen, C.-T. Liang, W.-H. Wang, *Sci. Rep.* **2015**, *5*, 11472.
- [13] S. Jeon, S.-E. Ahn, I. Song, C. J. Kim, U. I. Chung, E. Lee, I. Yoo, A. Nathan, S. Lee, K. Ghaffarzadeh, J. Robertson, K. Kim, *Nat. Mater.* **2012**, *11*, 301.
- [14] Y. Zhao, S. Bertolazzi, P. Samorì, *ACS nano* **2019**, *13*, 4814.
- [15] a) M. Gobbi, E. Orgiu, P. Samorì, *Adv. Mater.* **2018**, *30*, 1706103; b) A. K. Geim, I. V. Grigorieva, *Nature* **2013**, *499*, 419.
- [16] a) L. Liao, J. Bai, Y. Qu, Y.-c. Lin, Y. Li, Y. Huang, X. Duan, *Proc. Natl. Acad. Sci.* **2010**, *107*, 6711; b) L. Liao, Y.-C. Lin, M. Bao, R. Cheng, J. Bai, Y. Liu, Y. Qu, K. L. Wang, Y. Huang, X. Duan, *Nature* **2010**, *467*, 305.
- [17] N. Mitoma, Y. Yano, H. Ito, Y. Miyauchi, K. Itami, *ACS Appl. Nano Mater.* **2019**, *2*, 4825.

- [18] a) M. Gobbi, S. Bonacchi, J. X. Lian, A. Vercouter, S. Bertolazzi, B. Zyska, M. Timpel, R. Tatti, Y. Olivier, S. Hecht, M. V. Nardi, D. Beljonne, E. Orgiu, P. Samorì, *Nat. Commun.* **2018**, *9*, 2661; b) E. Orgiu, N. Crivillers, M. Herder, L. Grubert, M. Pätzelt, J. Frisch, E. Pavlica, D. T. Duong, G. Bratina, A. Salleo, N. Koch, S. Hecht, P. Samorì, *Nat. Chem.* **2012**, *4*, 675; c) H. Qiu, Y. Zhao, Z. Liu, M. Herder, S. Hecht, P. Samorì, *Adv. Mater.* **2019**, *31*, 1903402.
- [19] H. Li, Q. Zhang, C. C. R. Yap, B. K. Tay, T. H. T. Edwin, A. Olivier, D. Baillargeat, *Adv. Funct. Mater.* **2012**, *22*, 1385.
- [20] B. Chakraborty, A. Bera, D. V. S. Muthu, S. Bhowmick, U. V. Waghmare, A. K. Sood, *Phys. Rev. B* **2012**, *85*, 161403.
- [21] K. F. Mak, K. He, C. Lee, G. H. Lee, J. Hone, T. F. Heinz, J. Shan, *Nat. Mater.* **2013**, *12*, 207.
- [22] J. Yuan, S. Najmaei, Z. Zhang, J. Zhang, S. Lei, P. M. Ajayan, B. I. Yakobson, J. Lou, *ACS nano* **2015**, *9*, 555.
- [23] M. M. Furchi, D. K. Polyushkin, A. Pospischil, T. Mueller, *Nano Lett.* **2014**, *14*, 6165.
- [24] a) B. Antonio Di, G. Luca, F. Tobias, G. Filippo, L. Giuseppe, C. Luca, L. Shi-Jun, L. K. Ang, S. Marika, *Nanotechnology* **2017**, *28*, 214002; b) D. J. Late, B. Liu, H. S. S. R. Matte, V. P. Dravid, C. N. R. Rao, *ACS Nano* **2012**, *6*, 5635.
- [25] S. Bertolazzi, M. Gobbi, Y. Zhao, C. Backes, P. Samorì, *Chem. Soc. Rev.* **2018**, *47*, 6845.
- [26] H. Fang, M. Tosun, G. Seol, T. C. Chang, K. Takei, J. Guo, A. Javey, *Nano Lett.* **2013**, *13*, 1991.

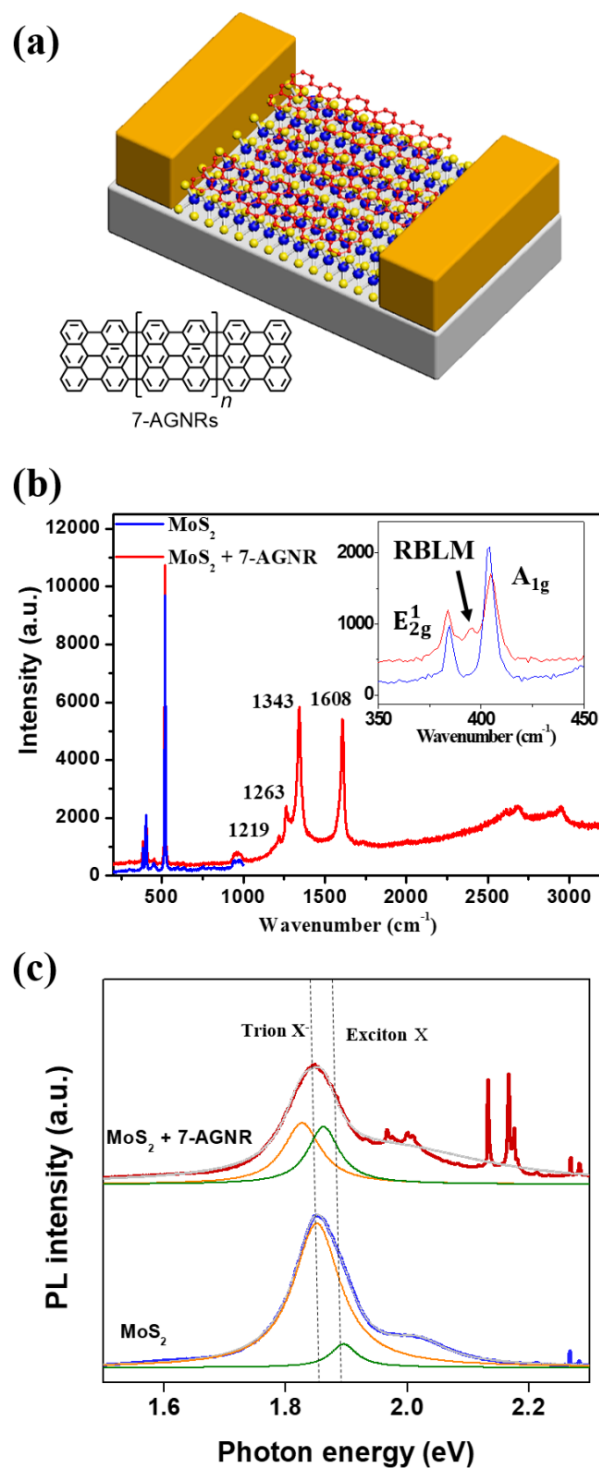


Figure 1. Van der Waals heterostructures based on MoS₂-GNR. (a) Schematic illustration of the FET device configuration based on MoS₂-GNR, with the molecular structures of employed 7-AGNR. (b) Raman and (c) Photoluminescence spectroscopy characterization of MoS₂ and MoS₂-GNR, respectively.

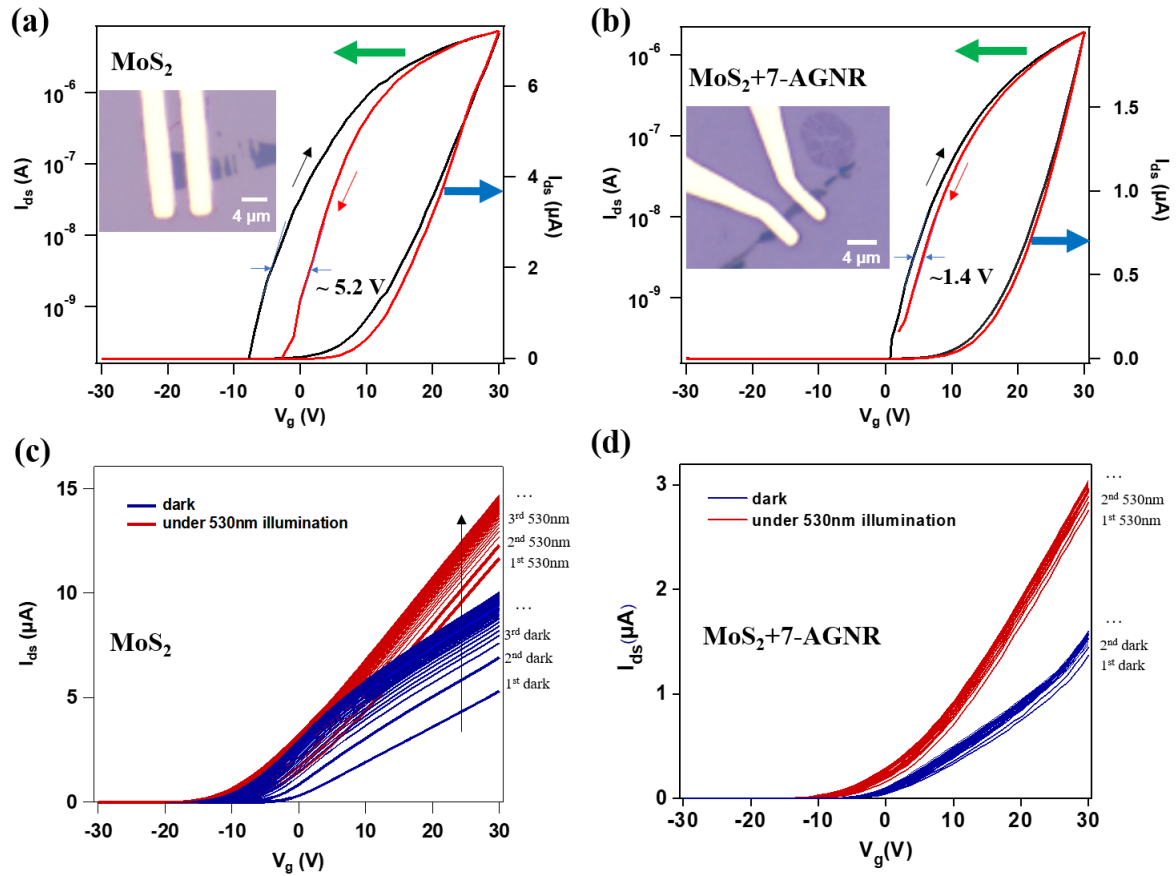


Figure 2. (a) and (b) Hysteresis test of FETs based on (a) pristine MoS₂ and (b) MoS₂-GNR VDWH, in both linear and logarithmic scale as indicated by the blue and green arrows, under dark condition. Inset shows the digital pictures of the FET devices. (c) and (d) Transfer characteristics of FETs based on (c) pristine MoS₂ and (d) MoS₂-GNR VDWH, under dark and 530 nm illumination conditions over 50 cycles.

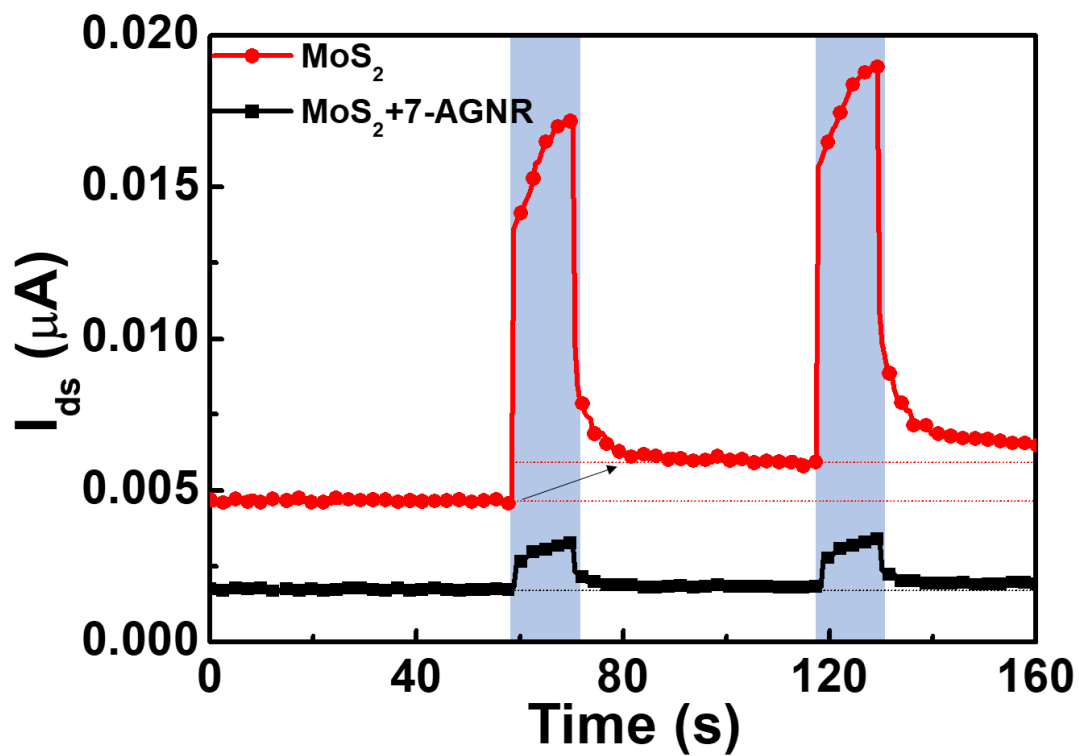


Figure 3. Comparison of the dynamic photoresponse of source-drain current upon 530 nm illumination (blue box area) between FETs based on pristine MoS_2 (red curve) and MoS_2 -GNR VDWH (black curve), $V_g = 0$ V.

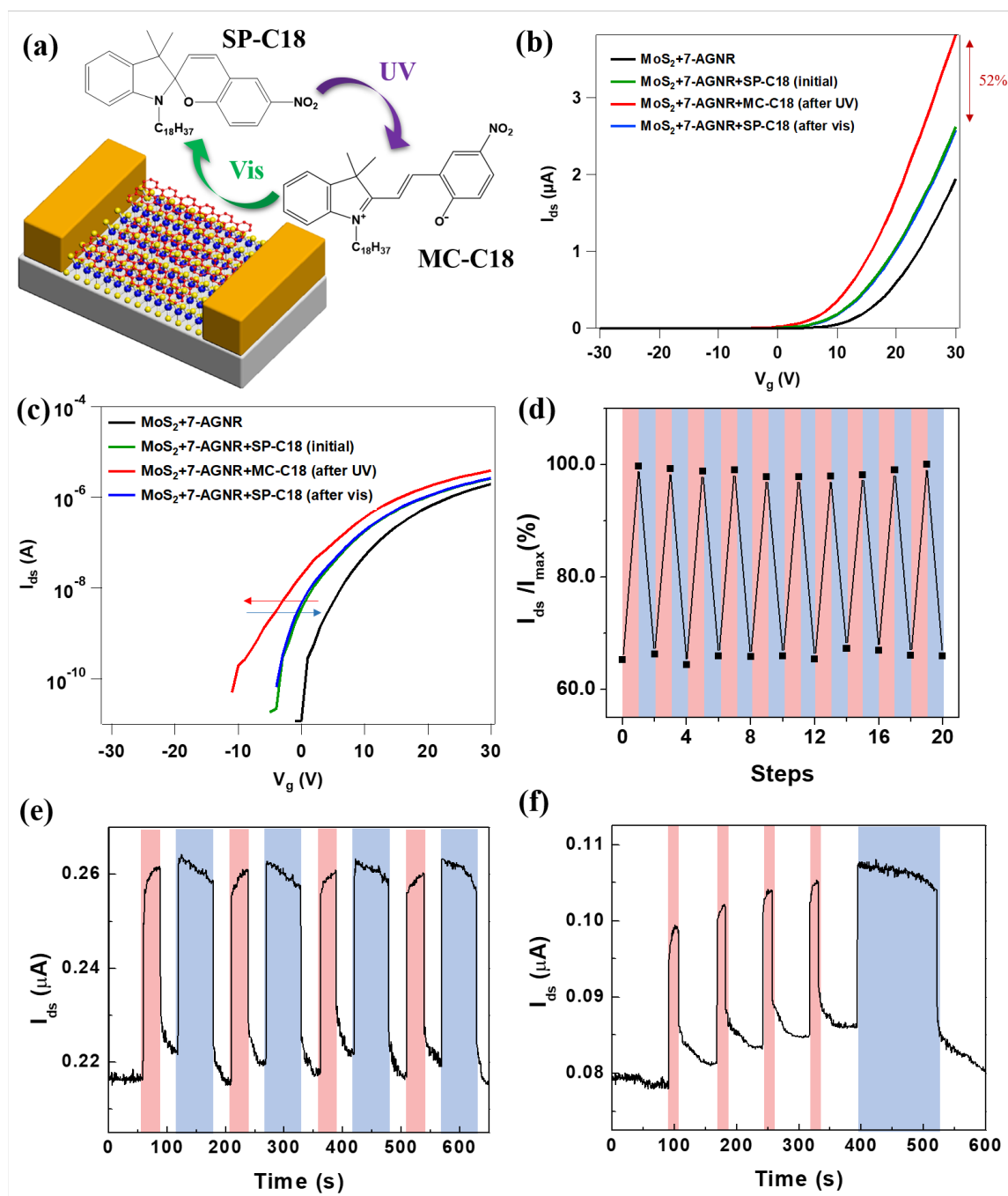


Figure 4. (a) Schematic illustration of the FET device architecture based on MoS₂-GNR with SP-C18 molecules. (b) and (c) Transfer evolution of the device before and after SP-C18 molecules deposition and after UV/vis illumination in (b) linear and (c) logarithm scale. (d) Current modulation with SP-C18 and MC-C18 isomers over ten illumination cycles of alternating UV (red boxed region) and visible (blue boxed region) light irradiation. All current values are normalized to the initial value obtained from the MC-C18 isomers. The connecting

lines are used as guides to the eye. (e) Dynamic current variation over alternative dark and UV/vis illumination conditions during four cycles. (f) Dynamic current variation under periodic UV illumination. Four distinct current levels can be achieved by short-time UV illumination and the current can be recovered by subsequent long-time vis illumination.